Ministry of Science and Higher Education of the Republic of Kazakhstan
SDU University

SDU
1996
UNIVERSITY

Yerimbet Aitzhanov

Global stability of dynamical systems and Lyapunov functions

THESIS

Presented in Partial Fulfillment for the
Degree of Master of Science in Mathematics
(degree code: 7M05401)
Department of Mathematics and Natural Sciences
Faculty of Engineering and Natural Sciences

Supervisor: **Shirali Kadyrov, PhD**

Kaskelen, June 2024

SDU University
Faculty of Engineering and Natural Sciences
Department of Mathematics and Natural Sciences

Dean of Faculty of Engineering and Natural Sciences

Assistant Professor, Ph.D. Akhmedov Ramis

« 4 » June 2024

Topic of the thesis:

Global stability of dynamical systems and Lyapunov functions

Thesis submitted as part of the requirements for the award of the MSc in "7M05401-Mathematics"

Head of Department Birzhan Ayanbayev, PhD

Academic Supervisor Shirali Kadyrov, PhD

Master student Yerimbet Aitzhanov

Kaskelen, 2024

Declaration

I confirm that this is my own work and the use of all material from other sources has been properly and fully acknowledged.

Yerimbet Aitzhanov

June 2024

Acknowledgements

I would like to thank my supervisor prof. Shirali Kadyrov and all SDU staff of department of Mathematics for supporting and advising.

Dedication

This thesis is dedicated to:

My parents, SDU, NU and many other for their support, help and useful comments for improving this project.

Abstract

In this study, we explore the global stability of a novel epidemic model that integrates reported and unreported cases, distinguishing between symptomatic and asymptomatic individuals. Using a Lyapunov function, we demonstrate the model's stability, highlighting the crucial role of asymptomatic cases in shaping disease dynamics and control effectiveness. Furthermore, we perform a novel hybrid parameter estimation method based on genetic algorithms, utilizing COVID-19 data from the UK to better understand the distribution of reported and unreported cases in the early phases of an epidemic. In addition, we employ sensitivity analysis to understand the impact of this division on the fundamental reproduction number. Our findings underscore the importance of accounting for both symptomatic and asymptomatic cases in epidemic modeling and control strategies.

Аңдатпа

Бұл зерттеуде біз симптоматикалық және симптомсыз адамдарды ажырата отырып, хабарланған және хабарланбаған жағдайларды біріктіретін жаңа эпидемиялық модельдің жаһандық тұрақтылығын зерттейміз. Ляпунов функциясын пайдалана отырып, біз модельдің тұрақтылығын көрсетеміз, аурудың динамикасы мен бақылау тиімділігін қалыптастырудағы асимптоматикалық жағдайлардың шешуші рөлін атап өтеміз. Сонымен қатар, біз эпидемияның бастапқы фазаларында хабарланған және хабарланбаған жағдайлардың таралуын жақсырақ түсіну үшін Ұлыбританиядан алынған COVID-19 деректерін пайдалана отырып, генетикалық алгоритмдерге негізделген жаңа гибридті параметрлерді бағалау әдісін орындаймыз. Бұған қоса, біз бұл бөлудің негізгі көбею санына әсерін түсіну үшін сезімталдық талдауын қолданамыз. Біздің қорытындыларымыз эпидемиялық модельдеу және бақылау стратегияларында симптоматикалық және асимптоматикалық жағдайларды есепке алудың маңыздылығын көрсетеді.

Аннотация

В этом исследовании мы изучаем глобальную стабильность новой модели эпидемии, которая объединяет зарегистрированные и незарегистрированные случаи, различая людей с симптомами и бессимптомными. Используя функцию Ляпунова, мы демонстрируем стабильность модели, подчеркивая решающую роль бессимптомных случаев в формировании динамики заболевания и эффективности контроля. Кроме того, мы применяем новый гибридный метод оценки параметров, основанный на генетических алгоритмах, используя данные о COVID-19 из Великобритании, чтобы лучше понять распределение зарегистрированных и незарегистрированных случаев на ранних стадиях эпидемии. Кроме того, мы используем анализ чувствительности, чтобы понять влияние этого разделения на фундаментальный коэффициент воспроизводства. Наши результаты подчеркивают важность учета как симптоматических, так и бессимптомных случаев при моделировании эпидемии и стратегиях контроля.

Contents

Declaration i

Acknowledgements ii

Dedication iii

Abstract iv

1 Introduction 1

2 Literature review 4
2.1 Types of Lyapunov functions 4
2.2 Epidemic models 5
2.2.1 SIS model 5
2.2.2 SIR and SIRS models 7

3 Mathematical model formulation 10
3.1 The invariant set 11

4 Stability of the Disease Free Equilibrium 15
4.1 Basic reproduction number 15
4.2 Global Stability of Disease Free Equilibrium 16

5 Model parameter estimation 18
5.1 Methodology 18
5.2 Parameter estimation results 21

6 Sensitivity and elasticity analysis 26
6.1 Elasticity of $\mathcal{R}_0$ 26
6.2 Partial Rank Correlation Coefficient 27
6.3 Sobel index 28

7 Visualization 30

8 Conclusion 32

References **33**

1. Introduction

The field of biomathematics has experienced significant growth, particularly in the area of infectious disease transmission models. Infectious diseases pose significant challenges to public health systems worldwide, necessitating the development of sophisticated mathematical models to understand and control their impact. Traditional epidemic models, such as the Susceptible-Infected-Recovered (SIR) framework , have played a crucial role in understanding disease dynamics [1]. However, these models often overlook the subtle complexities associated with varying degrees of symptomatology and the presence of asymptomatic carriers. The COVID-19 pandemic has highlighted the significant role of asymptomatic individuals in disease transmission, necessitating their inclusion in epidemic modeling and control strategies [2]. This is particularly important given the potential for reduced transmission from asymptomatic cases and the challenges in identifying and isolating them [3]. Modeling efforts have shown that strict interventions are crucial to impede potential COVID-19 transmission, even after diagnosed patients are cured, to prevent a second outbreak [4].

In response to these challenges, recent research has emphasized the need for epidemic models that account for both symptomatic and asymptomatic individuals [5], as these subpopulations play different roles in disease transmission. Chen [6] and Bi [7] both developed compartmental models that explicitly incorporate these subpopulations, with Chen focusing on the impact of response measures and Bi on the role of asymptomatic carriers in disease spread recent research has focused on developing novel epidemic models that explicitly incorporate separate compartments for symptomatic and asymptomatic individuals. These models aim to provide a more accurate understanding of disease transmission dynamics by capturing the differential contributions of these subpopulations to overall disease spread. These studies collectively underscore the need for more detailed epidemic models that can better capture the complexities of disease transmission.

Central to the analysis of such models is the assessment of their global stability, which is crucial for predicting long-term epidemic outcomes and evaluating the efficacy of intervention strategies. A range of studies have addressed the challenge of conducting global stability analyses for complex epidemic models. Liao and Wang [8] introduced a method for analyzing the global stability

of high-dimensional nonlinear autonomous systems, while Tian and Wang [9] applied three different techniques to investigate the global stability of cholera epidemic models. Nabti and Ghanbari [10] explored the global stability of a fractional SVEIR model, focusing on the well-posedness of the model and the stability of its equilibrium points. More recent works employed various techniques to investigate the global stability of different types of epidemic models, including age-infection-structured SI model [11], SIRS pulse vaccination [12], SAIRS [13], SEIRS [14], and models incorporating latency and differential infectivity [15]. In particular, the SAIRS model developed by Ottaviano et al. [13], in which the model considers the roles of asymptomatic and symptomatic infected individuals, has been analyzed for its global stability. The study determined the basic reproduction number R_0, a key determinant of epidemic dynamics [16], and proved that the disease-free equilibrium is globally asymptotically stable if $R_0 < 1$. Similar findings are essential for predicting the long-term outcome of an epidemic and evaluating the effectiveness of interventions aimed at reducing the spread of the disease.

Previous models had limitations including the omission of the exposed compartment, failure to account for virus-induced mortality and dynamic population changes, and the occurrence of reinfections. In this paper, we aim to develop a more comprehensive model addressing these shortcomings, particularly in the context of scenarios like the COVID-19 pandemic. We contribute to this growing body of literature by presenting a global stability analysis of a novel epidemic model that integrates reported and unreported cases, distinguishing between symptomatic and asymptomatic individuals. Our approach is based on developing novel Lyapunov functions that have emerged as key tools in assessing the global stability of classical models, as demonstrated by studies conducted by Beretta and Takeuchi [17], Korobeinikov and Wake[18], and Gao et al.[19]. Building upon the foundational work in epidemic modeling, our model incorporates key features of disease transmission dynamics while addressing the limitations of existing approaches.

Furthermore, we extend our analysis beyond theoretical considerations by performing a novel hybrid parameter estimation method based on a heuristic approach. Using real-world COVID-19 data from the United Kingdom, we estimate the model parameters and provide insights into the distribution of reported and unreported cases during the early phases of an epidemic. This empirical validation enhances the applicability of our model and underscores its relevance for informing public health policy and intervention strategies. Last but not least, we employ sensitivity analysis techniques to explore the impact of individual parameters on partitioned compartments.

Our work contributes to a deeper knowledge of infectious disease dynamics and support evidence-based public health decision-making by clarifying the global stability of our unique epidemic model and offering insights into the dynamics of symptomatic and asymptomatic cases. In addition to highlighting

the need of strong mathematical frameworks in the fight against infectious illnesses, our study highlights the necessity of include both symptomatic and asymptomatic cases into epidemic models.

In the next section, we present the mathematical formulation of our model and discuss the invariance of the set we are interested in. Subsequently, we establish the global stability of the model, marking a significant advancement in the field of biomathematics. In Chapter 4, we derive a Lyapunov function for our SEIR-type Epidemic model and establish the global stability of the model. Chapter 5 presents the hybrid epidemiologic parameter estimation method and its application. In Chapter 6, we study sensitivity of the basic reproduction number to various parameter values. In Chapter 7, we make visualizations using as initial condition real situation's values. The article ends with conclusion and future directions.

Lyapunov stability theory was come out of Aleksandr Lyapunov, a Russian mathematician in 1892, and came from his doctoral dissertation. Until now, the theory of Lyapunov stability is still important to stability theory of dynamical systems.[20]

Knowing that dynamical system is global stable or not is very important, because for example we can decide is epidemic dangerous or not.

Definition 1.0.1 (Positive definite functions)**.** A function $V : R^n \to R$ is positive definite (PD) if

- $V(x) \geq 0$ for all x
- $V(x) = 0$ if and only if $x = 0$
- all sublevel sets of V are bounded

last condition equivalent to $V(x) \to \infty$ as $x \to \infty$

Theorem 1.0.2 (A Lyapunov global asymptotic stability theorem)**.** *Suppose there is a function V such that*

- *V is positive definite*
- *$\dot{V}(x) < 0$ for all $x \neq 0, \dot{V}(0) = 0$*

then, every trajectory of $\dot{x} = f(x)$ converges to zero as $t \to \infty$
(i.e., the system is globally asymptotically stable). Where $x = x(t)$; $\dot{x} = f(x)$. [21] [22]

2. Literature review

2.1 Types of Lyapunov functions

- The logarithmic Lyapunov function proposed by Goh for Lotka-Volterra systems:

$$L(x_1, x_2, \ldots, x_n\ ) = \Sigma_{i=1}^{n}\ c_i\ \left(x_i - x_i^* - x_i^*\ ln\frac{x_i}{x_i^*}\right)$$

  This function are derived from the primary integral of the well-known Lotka-Volterra prey-predator system and gained prominence through a series of publications by Bean-San Goh [23, 24, 25].

- Common quadratic Lyapunov function, have been extensively exploited for nonlinear and linear systems:

$$V(x_1, x_2, \ldots, x_n\ ) = \Sigma_{i=1}^{n}\ \ \frac{c_i}{2}\ (x_i - x_i^*\ )^2$$

- Composite quadratic function:

$$W(x_1, x_2, \ldots, x_n\ ) = \frac{c}{2}\ \left[\Sigma_{i=1}^{n}\ (x_i - x_i^*\ )\right]^2$$

- Linear combination of infectious compartments:

$$L(x_1, x_2, \ldots, x_n\ ) = \Sigma_{i\geq 2}^{n}\ c_i\ x_i$$

- Lyapunov functions are formulated as integrals encompassing the dynamics of the model. Typically, the integration interval initiates at a designated Endemic Equilibrium (EE) value x_i^* and concludes at the same x_i. This approach proves advantageous when ensuring the uniqueness of the EE is guaranteed, even though determining the precise values of the EE may pose analytical challenges. Integral Lyapunov functions prove particularly advantageous when the model involves multiple stages of infection, leading to a transition from an exponential distribution of the infectious period to a gamma distribution [26, 27, 28, 29, 30, 31]. These integral Lyapunov functions, albeit taking different forms, find widespread application in models featuring explicit delays, such as systems of Delay Differential Equations, and age-structured models.

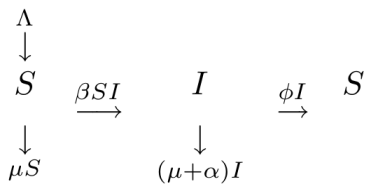

Figure 2.1: SIS model

2.2 Epidemic models

In this section, we use above mentioned types of Lyapunov functions to prove global stability of SIS, SIR and SIRS epidemic models [32].

2.2.1 SIS model

Certain diseases do not provide enduring immunity, leaving individuals susceptible to reinfection. These infections lack a recovered state, and individuals may become susceptible again after being infected. A suitable model for such diseases is the SIS type. In this model, the total population N is divided into two compartments, where N equals the sum of individuals in the susceptible class (S) and those who are infectious (I). The SIS model depicts a recurring cycle wherein individuals move from the susceptible state (S) to the infectious state (I) and back to the susceptible state (S), as illustrated in Figure 2.1.

The system of equations of model SIS [33]:

$$\begin{cases} \dfrac{dS}{dt} &= \Lambda - \beta SI - \mu S + \phi I \\ \dfrac{dI}{dt} &= \beta SI - (\phi + \mu + \alpha)I \end{cases} \tag{2.1}$$

The parameters in the model are positive constants. The constant Λ represents the recruitment rate of susceptibles, accounting for births and immigration, while μ denotes the per capita natural mortality rate. In our assumptions, a disease has the potential to be fatal for some infected individuals; therefore, we incorporate deaths due to the disease in the model using the disease-related death rate from the infectious class, denoted as α. Additionally, ϕ signifies the rate at which individuals move from the infectious class back to the susceptible class, without acquiring immunity.

The disease-free equilibrium (DFE) $E^0 = \left(S^0, I^0\right) = \left(\frac{\Lambda}{\mu}, 0\right)$ and basic reproduction number $\mathcal{R}_0 = \frac{\Lambda\beta}{\mu(\phi+\ \mu+\ \alpha)}$. Basic reproductive number was found by Next generation matrix method [34]. The term $\mathcal{R}_0$ is characterized as the mean count of secondary infections that arise when a single infectious individual is introduced to a host population that is entirely susceptible. Feasible region:

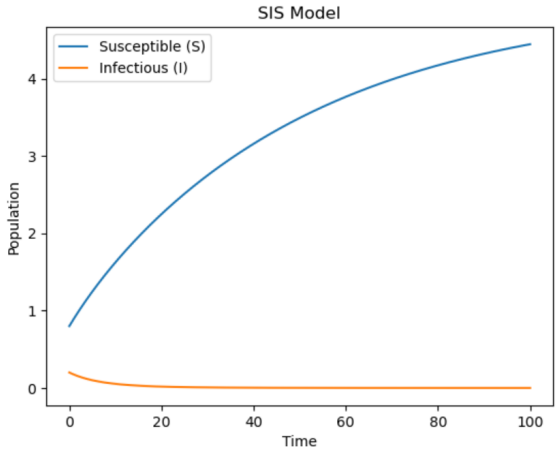

Figure 2.2: SIS model implementation in Python when $\mathcal{R}_0 \leq 1$

$G = \left\{(S, I) \in \mathbb{R}^2{}_+ : \quad S \geq 0, \quad I \geq 0, \quad S + I \leq \frac{\Lambda}{\mu}\right\}$ which is positively invariant with respect to SIS model's system of equations.

Theorem 2.2.1. *The DFE* E^0 *is globallsy asymptotically stable in* G *if* $\mathcal{R}_0 \leq 1$.

Proof. To prove it we can define $L : \{(S, I) \in G : S, I > 0\}$:

$$L(S, I) = \frac{1}{2}\left[\left(S - S^0\right) + I\right]^2 + \frac{\alpha + 2\mu}{\beta} I$$

Obviously, $L > 0$ and $L\left(S_0, I_0\right) = 0$. The time derivative of L is not positive if $\mathcal{R}_0 \leq 1$:

$$\frac{dL}{dt} = -\mu\left(S - S^0\right)^2 - (\mu + \alpha)I^2 - \frac{(\alpha + 2\mu)(\phi + \mu + \alpha)}{\beta}\left(1 - \mathcal{R}_0\right) I$$

Therefore, the DFE E^0 is globallsy asymptotically stable in G if $\mathcal{R}_0 \leq 1$. □

Let's consider endemic equilibtium (EE) of SIS model:

$$E^* = (S^*, I^*) = \left(\frac{S^0}{R^0}, \frac{\mu\left(\phi + \ \mu + \ \alpha\right)}{\beta\left(\alpha + 2\mu\right)}(\mathcal{R}_0 - 1)\right)$$

.

Theorem 2.2.2. *The EE* E^* *is globallsy asymptotically stable in* G *if* $\mathcal{R}_0 > 1$.

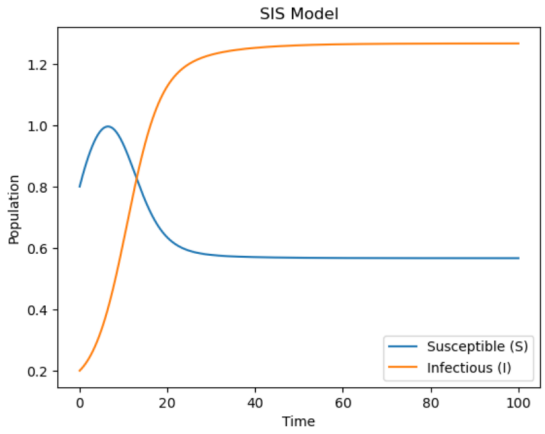

Figure 2.3: SIS model implementation in Python when $\mathcal{R}_0 > 1$

Proof. To prove it we can define function using combination of composite quadratic Lyapunov function and logarithmic Lyapunov function,

$$L : \{(S, I) \in G : S, I > 0\}$$

$$L(S, I) = \frac{1}{2}\left[(S - S^*) + (I - I^*)\right]^2 + \frac{\alpha + 2\mu}{\beta}\left(I - I^* - I^* \ln \frac{I}{I^*}\right)$$

Obviously, $L > 0$ and $L\left(S^*, I^*\right) = 0$. The time derivative of L is not positive if $\mathcal{R}_0 > 1$:

$$\frac{dL}{dt} = -\mu\left(S - S^*\right)^2 - (\mu + \alpha)\left(I - I^*\right)^2$$

Therefore, the EE E^* is globally asymptotically stable in G if $\mathcal{R}_0 > 1$. □

2.2.2 SIR and SIRS models

Certain infectious diseases provide lasting immunity, while others confer temporary acquired immunity. These two types of diseases can be represented by the SIR model for permanent immunity and the SIRS model for temporary acquired immunity. The total population N is divided into three compartments, where N equals the sum of individuals in the susceptible class (S), infectious individuals (I), and those who have recovered (R). The system of equations of model SIR [33]:

$$\begin{cases} \dfrac{dS}{dt} = \Lambda - \beta SI - \mu S + \gamma R \\ \dfrac{dI}{dt} = \beta SI - (\kappa + \mu + \alpha)I \\ \dfrac{dR}{dt} = \kappa I - (\mu + \gamma)R \end{cases}$$

In this context, the parameters Λ, μ, β, κ, and α are positive constants, while γ is a non-negative constant. We assume that κ denotes the rate at

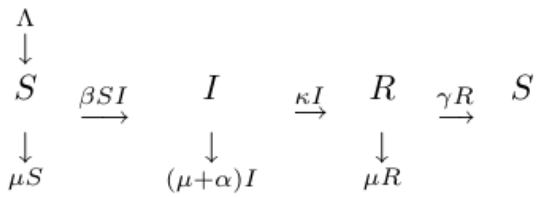

Figure 2.4: SIR and SIRS model

which infectives recover. When individuals who have recovered gain permanent immunity ($\gamma = 0$), we have the SIR model. Conversely, when individuals acquire temporary immunity ($\gamma \neq 0$), it corresponds to the SIRS model.

The disease-free equilibrium (DFE) $\mathrm{E}^0 = \left(S^0, I^0, R^0\right) = \left(\frac{\Lambda}{\mu}, 0, 0\right)$ and basic reproduction number $\mathcal{R}_0 = \frac{\Lambda\beta}{\mu(\phi+\mu+\alpha)}$. Feasible region is:

$$G = \left\{(S, I, R) \in \mathbb{R}^3{}_+ : S \geq 0, I \geq 0, R \geq 0, S + I + R \leq \frac{\Lambda}{\mu}\right\}$$

which is positively invariant with respect to SIR and SIRS model's system of equations.

Theorem 2.2.3. *The DFE E^0 is globally asymptotically stable in G if $\mathcal{R}_0 \leq 1$.*

Proof. To prove it we can define $L : \{(S, I, R) \in G : S, I, R > 0\}$:

$$L(S, I, R) = \frac{1}{2}\left[\left(S - S^0\right) + I + R\right]^2 + \frac{\alpha + 2\mu}{\beta} I + \frac{\alpha + 2\mu}{2\kappa} R^2$$

Obviously, $L > 0$ and $L\left(S^0, I^0\right) = 0$. The time derivative of L is not positive if $\mathcal{R}_0 \leq 1$:

$$\frac{dL}{dt} = -\mu\left[\left(S - S^0\right) + R\right]^2 - (\mu + \alpha)I^2 - \frac{(\alpha + 2\mu)(\mu + \gamma)}{\kappa} R^2$$
$$- \frac{(\alpha + 2\mu)(\phi + \mu + \alpha)}{\beta}\left(1 - \mathcal{R}_0\right) I$$

Therefore, the DFE E^0 is globally asymptotically stable in G if $\mathcal{R}_0 \leq 1$. □

Let's consider the endemic equilibrium (EE) of SIR and SIRS model:

$$\mathrm{E}^* = (S^*, I^*, R^*) = \left(\frac{S^0}{R^0}, \frac{\mu(\mu + \gamma)(\kappa + \alpha + \mu)\left(\mathcal{R}_0 - 1\right)}{\beta(\kappa\mu + (\mu + \gamma)(\alpha + \mu))}, \frac{\kappa\mu(\kappa + \alpha + \mu)\left(\mathcal{R}_0 - 1\right)}{\beta(\kappa\mu + (\mu + \gamma)(\alpha + \mu))}\right).$$

Theorem 2.2.4. *The EE E^* is globally asymptotically stable in* G *if $\mathcal{R}_0 > 1$.*

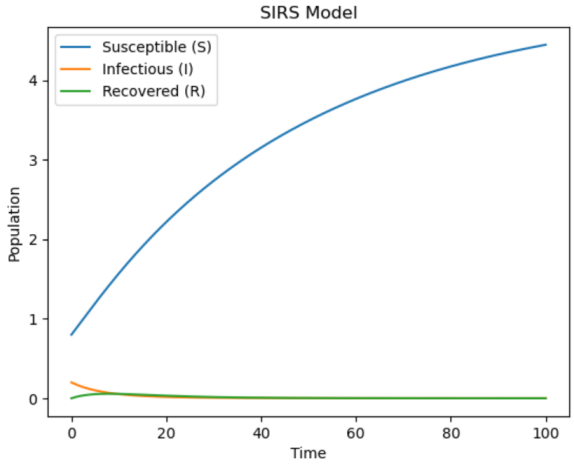

Figure 2.5: SIRS model implementation in Python when $\mathcal{R}_0 \leq 1$

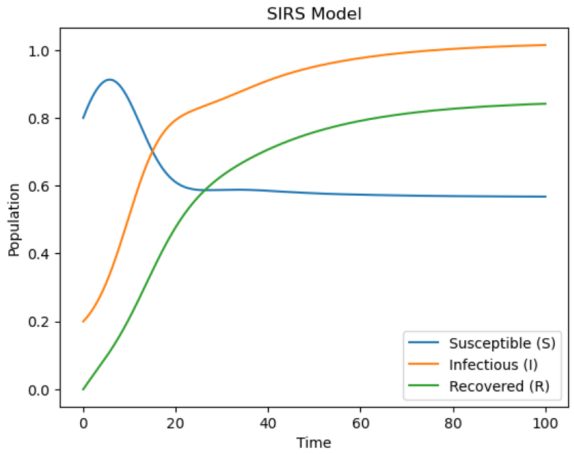

Figure 2.6: SIRS model implementation in Python when $\mathcal{R}_0 > 1$

Proof. To prove it we can define function using combination of composite quadratic Lyapunov function and logarithmic Lyapunov function,

$$L : \{(S, I, R) \in G : S, I, R > 0\}$$

$$L(S, I, R) = \frac{1}{2}\left[(S - S^*) + (I - I^*) + (R - R^*)\right]^2 + \frac{\alpha + 2\mu}{\beta}\left(I - I^* - I^* \ln \frac{I}{I^*}\right)$$
$$+ \frac{\alpha + 2\mu}{2\kappa}\left(R - R^*\right)^2$$

Obviously, $L > 0$ and $L\left(S^*, I^*, R^*\right) = 0$. The time derivative of L is not positive if $\mathcal{R}_0 > 1$:

$$\frac{dL}{dt} = -\mu\left[(S - S^*) + (R - R^*)\right]^2 - (\mu + \alpha)\left(I - I^*\right)^2$$
$$- \frac{(\alpha + 2\mu)(\mu + \gamma)}{\kappa}\left(R - R^*\right)^2$$

Therefore, the EE* is globally asymptotically stable in G if $\mathcal{R}_0 > 1$. □

3. Mathematical model formulation

In this chapter we introduce our model and study invariance. Some very recent models take into account the asymptomatic cases. This is a significant development in understanding the spread of COVID-19, as these carriers can transmit the virus without showing symptoms, complicating efforts to control the pandemic. [35] highlights a case study where an asymptomatic carrier from Wuhan traveled to Anyang and interacted with a family, leading to five members developing COVID-19 pneumonia. This study underscores the potential for asymptomatic carriers to contribute to the spread of the virus, even when standard diagnostic imaging does not reveal signs of infection. [36] introduce a novel θ-SEIHRD model which is distinct from general-purpose models like SIR or SEIR as it incorporates the fraction θ of detected cases over the total real infected cases. This allows for the analysis of the impact of detection rates on the spread of COVID-19 and the estimation of hospital bed needs. While they provide formula for basic reproduction number, they do not study global stability. In their paper [37] discuss the SAIR model, which includes a compartment for asymptomatic individuals who can infect others. This model suggests that herd immunity could be achieved with a lower percentage of infected individuals than previously thought and highlights the effectiveness of lockdowns in controlling disease spread. Lastly, [13] provides a global stability analysis of an SAIRS-type epidemic model that includes vaccination and differentiates between asymptomatic and symptomatic infectious individuals in the disease transmission patterns.

We observe that previous SAIR-type models, which have been discussed above and include asymptomatic cases, have omitted the exposed (E) compartment. However, in many scenarios, such as with COVID-19, the virus has an incubation period, making it imperative not to disregard E. Moreover, these models fail to explicitly consider virus-induced mortality. Another limitation is their assumption of a constant population, which does not hold true for the prolonged duration of the COVID-19 pandemic. Finally, due to the extended timeframe, instances of reinfection occur due to waning immunity. Bearing all these factors in mind, we will now develop a more realistic model.

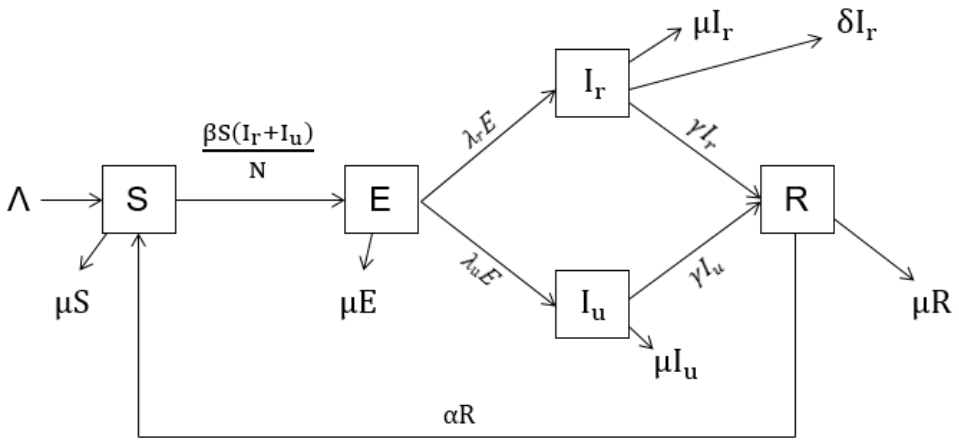

Figure 3.1: SEIR model version accounting reported and unreported cases.

The model subdivides the total population, $N(t)$, into susceptible $S(t)$, exposed $E(t)$, reported (symptomatic) infected $I_r(t)$, unreported (asymptomatic) infected $I_u(t)$, and recovered $R(t)$, so that:

$$N(t) = S(t) + E(t) + I_r(t) + I_u(t) + R(t).$$

Then the following epidemiological model whose the flow diagram is depicted in Figure 3.1 is formulated as follows.

$$\begin{cases} \dfrac{dS}{dt} = \Lambda - \dfrac{\beta S(I_r + I_u)}{N} - \mu S + \alpha R \\ \dfrac{dE}{dt} = \dfrac{\beta S(I_r + I_u)}{N} - \lambda_r E - \lambda_u E - \mu E \\ \dfrac{dI_r}{dt} = \lambda_r E - \gamma I_r - \delta I_r - \mu I_r \\ \dfrac{dI_u}{dt} = \lambda_u E - \gamma I_u - \mu I_u \\ \dfrac{dR}{dt} = \gamma I_r + \gamma I_u - \mu R - \alpha R \end{cases} \tag{3.1}$$

The parameters used in the model are summarized in Table 3.1.

3.1 The invariant set

To ensure the practical relevance and validity of our model, we establish a crucial lemma regarding the positivity of key variables. The lemma below emphasizes the non-negativity of the initial conditions and establishes that this

Parameter	Description
Λ	Recruitment rate of susceptible individuals through birth or immigration
β	Infection transmission rate
μ	Natural death rate
δ	Death rate due to the virus
γ	Recovery rate
α	Rate of loosing immunity
λ_r	Incubation-adjusted symptomatic (reported) rate
λ_u	Incubation-adjusted asymptomatic (unreported) rate
N	Constant initial population size ($N = N(0)$)

Table 3.1: Parameters and Descriptions.

property persists throughout the entire solution space of the system. This assurance is fundamental in affirming the meaningful interpretation of our model in real-world scenarios.

Lemma 3.1.1. *Let initial conditions for the model be positive* $S(0) \geq 0$, $E(0) \geq 0$, $I_r(0) \geq 0$, $I_u(0) \geq 0$, $R(0) \geq 0$, *then the variables of the model* $S(t)$, $E(t)$, $I_r(t)$, $I_u(t)$, $R(t)$ *will remain positive for all solutions of system* (3.1) *for all* $t > 0$.

Proof. Let $T = sup\{\tau \geq 0 | \forall 0 \leq t \leq \tau$ such that $S(t) \geq 0, E(t) \geq 0, I_r(t) \geq 0, I_u(t) \geq 0, R(t) \geq 0\}$. Let's prove that $\tau = +\infty$.

Suppose that $0 < T < +\infty$ then by the continuity of solutions we will have: $S(T) = 0$ or $E(T) = 0$ or $I_r(T) = 0$ or $I_u(T) = 0$ or $R(T) = 0$. There is 5 cases. If S becomes zero at time T, $S(t) = 0$, before $E(t)$, $I_r(t)$, $I_u(t)$, $R(t)$ become zero then:

$$S(T) = 0 \implies \frac{dS(T)}{dt} = \lim_{t \to T^-} \frac{S(T) - S(t)}{T - t} = \lim_{t \to T^-} \frac{-S(t)}{T - t} \leq 0$$

But from the first equation of system (3.1) with $S(T) = 0$ we have $\frac{dS(T)}{dt} = \Lambda > 0$.

Similarly, if $E(T)$ becomes zero at time T, before $S(t)$, $I_r(t)$, $I_u(t)$, $R(t)$ then:

$$E(T) = 0 \implies \frac{dS(E)}{dt} = \lim_{t \to T^-} \frac{E(T) - E(t)}{T - t} = \lim_{t \to T^-} \frac{-E(t)}{T - t} \leq 0$$

From the second equation of system (3.1) with $E(T) = 0$ we have $\frac{dE(T)}{dt} =$

$\frac{\beta S(I_r + I_u)}{N}$. Since β is the infection rates between susceptible and infectious individuals, hence $\beta > 0$. And $\frac{S(I_r + I_u)}{N}$ is strictly positive at the moment T, as noted above. So, $\frac{dE(T)}{dt} = \frac{\beta S(I_r + I_u)}{N} > 0$.

Similar proof for $I_r(t)$, $I_u(t)$, $R(t)$. So T could not be finite, which concludes the proof.

□

In the analysis of our model, we establish the positive invariance of a closed set, crucial for understanding the system's dynamics.

Proposition 3.1.2. *The closed set*

$$\mathcal{G} = \{(S, E, I_r, I_u, R) \in \mathbb{R}^5_+ \text{ such that } S + E + I_r + I_u + R \leq \frac{\Lambda}{\mu}\}$$

is positively invariant.

Proof. Adding all the equations of the model 3.1 gives,

$$\frac{dN}{dt} = \Lambda - \mu N - \delta I_r$$

Obviously, it implies:

$$\frac{dN}{dt} \leq \Lambda - \mu N$$

To prove that G is positively invariant, we should prove following:
If $N(0) < \frac{\Lambda}{\mu} \implies N(t) < \frac{\Lambda}{\mu}, \forall t \geq 0$
By contradiction, assume not. $\exists t : N(t) \geq \frac{\Lambda}{\mu}$, so if we define a set

$$S = \{t : N(t) \geq \frac{\Lambda}{\mu}\} = N^{-1}[\frac{\Lambda}{\mu}, \infty),$$

then clearly it is not empty.

Since $N(t)$ is continued function function on $[0, \infty)$, it follows that the set S is closed. Since, by Lemma 3.1.1 $N(t) \geq 0$ we also know that S is bounded from below, hence it has infimum, say at $t_0 = \inf S$. In particular, for all $t \in [0, t_0)$ we have $N(t) < \frac{\Lambda}{\mu}$ and $N(t_0) \geq \frac{\Lambda}{\mu}$.

$0 \leq t \leq t_0 \quad \frac{dN(t)}{dt} \leq \Lambda - \mu N$

$$\frac{dN(t)}{\Lambda - \mu N(t)} \leq dt$$

$$\int_{N(0)}^{N(t_0)} \frac{dN(t)}{\Lambda - \mu N(t)} \leq \int_0^{t_0} dt$$

$$\frac{\ln|\Lambda-\mu N(t_0)|-\ln|\Lambda-\mu N(0)|}{-\mu}\leq t_0$$

$$\frac{\ln\left|\frac{\Lambda-\mu N(t_0)}{\Lambda-\mu N(0)}\right|}{-\mu}\leq t_0$$

By multiplying both sides to $-\mu$ we got:

$$\ln\left|\frac{\Lambda-\mu N(t_0)}{\Lambda-\mu N(0)}\right|\geq -\mu t$$

Then by taking exponent of both sides we got:

$$\frac{\Lambda-\mu N(t_0)}{\Lambda-\mu N(0)}\geq e^{-\mu t}$$

$$\Lambda-\mu N(t_0)\geq(\Lambda-\mu N(0))e^{-\mu t}$$

$$N(t_0)\leq\frac{\Lambda}{\mu}-\frac{(\Lambda-\mu N(0))e^{-\mu t}}{\mu}<\frac{\Lambda}{\mu}$$

This contradicts to $N(t_0)\geq\frac{\Lambda}{\mu}$.

Thus, the region $\mathcal{G}$ is positively invariant. Further, if $N(0)>\frac{\Lambda}{\mu}$, then either the solution enters $\mathcal{G}$ infinite time or $N(t)$ approaches $\frac{\Lambda}{\mu}$ asymptotically. Hence, the region $\mathcal{G}$ attracts all solutions in $\mathbb{R}^5_+$. □

4. Stability of the Disease Free Equilibrium

In this chapter we study global stability of the Disease Free equilibrium point ε_0 using Lyapunov method.

The system has an unique Disease Free Equilibrium (DFE) given by:

$$\varepsilon_0 = (S^*, E^*, I_r^*, I_u^*, R^*) = (\frac{\Lambda}{\mu}, 0, 0, 0, 0) \tag{4.1}$$

4.1 Basic reproduction number

To calculate the basic reproduction number $\mathcal{R}_0$, we use the next generation matrix FV^{-1} [34]:

$$\mathcal{R}_0 = \rho(\mathbf{FV^{-1}}) \tag{4.2}$$

Where F is nonnegative matrix of the new infection terms, and V is M-matrix of the transition terms associated with model (3.1),

$$\mathcal{F} = \begin{pmatrix} \frac{\beta S(I_r+I_u)}{N} \\ 0 \\ 0 \end{pmatrix}, \mathcal{V} = \begin{pmatrix} (\lambda_r + \lambda_u + \mu)E \\ -\lambda_r E + I_r(\gamma + \delta + \mu) \\ -\lambda_u E + I_u(\gamma + \mu) \end{pmatrix}$$

The infected compartments are E, I_r and I_u. Thus,

$$\mathbf{F} = \begin{pmatrix} 0 & \frac{\beta S^*}{N} & \frac{\beta S^*}{N} \\ 0 & 0 & 0 \\ 0 & 0 & 0 \end{pmatrix}, \mathbf{V} = \begin{pmatrix} \lambda_r + \lambda_u + \mu & 0 & 0 \\ -\lambda_r & \gamma + \delta + \mu & 0 \\ -\lambda_u & 0 & \gamma + \mu \end{pmatrix}$$

So FV^{-1} is given as:

$$\mathbf{FV^{-1}} = \begin{pmatrix} \frac{\beta S^*}{N(\lambda_r+\lambda_u+\mu)} \left(\frac{\lambda_r}{\mu+\gamma+\delta} + \frac{\lambda_u}{\mu+\gamma}\right) & \frac{\beta S^*}{N(\gamma+\delta+\mu)} & \frac{\beta S^*}{N(\gamma+\mu)} \\ 0 & 0 & 0 \\ 0 & 0 & 0 \end{pmatrix}$$

Hence, using formula (4.2) and remembering (4.1), we find out that the basic reproduction number is given by:

$$\mathcal{R}_0 = \frac{\beta\Lambda}{N\mu(\lambda_r + \lambda_u + \mu)}\left(\frac{\lambda_r}{\mu+\gamma+\delta} + \frac{\lambda_u}{\mu+\gamma}\right)$$

4.2 Global Stability of Disease Free Equilibrium

In our exploration of the system dynamics, we arrive at a significant result concerning the stability of the disease-free equilibrium. The following theorem establishes the global asymptotic stability of ε_0 under the condition $\mathcal{R}_0 < 1$.

Theorem 4.2.1. *For $\mathcal{R}_0 < 1$, the disease free equilibrium ε_0 of the system 3.1 is globally asymptotically stable (GAS) on $\mathcal{G} = \{(S, E, I_r, I_u, R) \in \mathbb{R}^5_+$ such that $S+ E + I_r + I_u + R \leq \frac{\Lambda}{\mu}\}$.*

Proof. Consider the following candidate for a Lyapunov function on $\mathcal{G}$

$$V(S, E, I_r, I_u, R) = aE + bI_r + cI_u, \tag{4.3}$$

where

$$\begin{aligned} a &= \frac{1}{(\lambda_r + \lambda_u + \mu)}\left(\frac{\lambda_r}{\mu+\gamma+\delta} + \frac{\lambda_u}{\mu+\gamma}\right), \\ b &= \frac{1}{\mu+\gamma+\delta}, \\ c &= \frac{1}{\mu+\gamma}. \end{aligned}$$

We first show that V is non-negative for all (S, E, I_r, I_u, R). At the disease-free equilibrium (DFE), ε_0, it is clear that $V(\varepsilon_0) = 0$. To establish that $V > 0$ for all $(S, E, I_r, I_u, R) \neq (\frac{\Lambda}{\mu}, 0, 0, 0, 0)$, note that all constants and (S, E, I_r, I_u, R) are positive. Hence, $V(S, E, I_r, I_u, R) > 0$ for all $(S, E, I_r, I_u, R) \neq (\frac{\Lambda}{\mu}, 0, 0, 0, 0)$.

Hence:

$$V(S, E, I_r, I_u, R) > 0 \text{ for all } (S, E, I_r, I_u, R) \neq (\frac{\Lambda}{\mu}, 0, 0, 0, 0)$$

Taking the time derivative of $V(t)$, we have:

$$\dot{V}(S, E, I_r, I_u, R) = a\frac{d}{dt}E(t) + b\frac{d}{dt}I_r(t) + c\frac{d}{dt}I_u(t)$$

Then, by substituting $(\dot{S}, \dot{E}, \dot{I}_r, \dot{I}_u, \dot{R})$ from (3.1) we have:

$$\dot{V}(S,E,I_r,I_u,R) = a\left(\frac{\beta S(I_r+I_u)}{N} - (\lambda_r+\lambda_u+\mu)E\right) + b\left(\lambda_r E - (\gamma+\delta+\mu)I_r\right) + c\left(\lambda_u E - (\gamma+\mu)I_u^*\right)$$

Recalling $S \leq \Lambda/\mu$ and simplifying we get

$$\dot{V}(S,E,I_r,I_u,R) \leq (I_r+I_u)\mathcal{R}_0 - \left(\frac{\lambda_r}{\mu+\gamma+\delta} + \frac{\lambda_u}{\mu+\gamma}\right)E + \left(\frac{\lambda_r}{\mu+\gamma+\delta} + \frac{\lambda_u}{\mu+\gamma}\right)E + (I_r+I_u)$$

By reducing left elements that we can reduce and by bracketing identical elements

$$\dot{V}(S,E,I_r,I_u,R) = (I_r+I_u)(\mathcal{R}_0-1)$$

When $\mathcal{R}_0 < 1$, we have $\dot{V} < 0$ proving the global stability. □

5. Model parameter estimation

In this chapter, we consider parameter estimation for the proposed SEI_rI_uR model.

5.1 Methodology

To fit the model to empirical data, we use COVID-19 data sourced from the United Kingdom (UK), aiming to estimate the parameters β, γ, λ_r, λ_u, and δ. Our analysis is centered on a 60-day period spanning from February 2, 2020, to March 31, 2020, employing the "Confirmed cases" dataset from the UK [38]. The total population (N) under consideration is 67,330,000. We set the values of μ and α to 0.000026 and 0.7, respectively, [39]. Given the relatively short time frame of 60 days, we assume a constant population, effectively setting Λ as the product of μ and N. Our initial conditions are defined as follows: $S_0 = N - 2$, $E_0 = 0$, $I_{r_0} = 2$, $I_{u_0} = 0$, $R_0 = 0$, and $C_0 = 2$.

Since the parameters β, γ, λ_r, λ_u, δ we want to estimate all lie in $(0, 1)$ we consider constraint optimization methodology. To this end, we employ two standard minimization algorithms and heuristic hybrid approaches as we now explain. We use the standard Nelder-Mead (NM) and Limited-memory Broyden–Fletcher–Goldfarb–Shanno with Box constraints (L-BFGS-B) methods. The Nelder-Mead method is a simplex-based optimization technique used for unconstrained optimization of nonlinear functions. It does not require gradient information and works by iteratively refining a simplex, a geometrical figure composed of $n+1$ vertices in an n-dimensional space. This method adjusts the simplex according to function evaluations at its vertices, employing operations such as reflection, expansion, contraction, and shrinkage to converge to a local minimum. The Limited-memory Broyden–Fletcher–Goldfarb–Shanno with Box constraints (L-BFGS-B) method is an optimization algorithm designed for large-scale problems. It is a quasi-Newton method that approximates the Broyden–Fletcher–Goldfarb–Shanno (BFGS) algorithm using limited memory, making it suitable for problems with a large number of variables. This method supports bound constraints on the variables and uti-

lizes gradient information to iteratively update the solution, balancing between convergence speed and memory efficiency. These methods were applied with bounds set to $(0, 1)$ and initial conditions (x_0) for the minimize function as $[\beta, \gamma, \lambda_r, \lambda_u, \delta] = [0.1, 0.1, 0.1, 0.1, 0.1]$.

For the heuristic hybrid approach, we employ both the Nelder-Mead followed by Genetic Algorithm (NM-GA) and the Genetic Algorithm followed by Nelder-Mead (GA-NM). A Genetic Algorithm (GA) is a heuristic optimization technique that operates on a population of candidate solutions, applying operators such as selection, crossover (recombination), and mutation to evolve better solutions over successive generations. GAs are particularly useful for complex optimization problems where the search space is large and the objective function may be non-differentiable or multimodal. To compare the methods, each code was run 5 times, and the minimum Loss (RMSE) value from these runs was used. Additionally, we used hybrid methods, where the genetic algorithm's estimated values served as the initial condition for Nelder-Mead (GA-NM), and conversely, the Nelder-Mead results were used as the starting point for the Genetic Algorithm (NM-GA).

In the GA implementation, we utilize 2 children generated through crossover with a crossover point set at bit 50. Parameters are encoded as binary strings, with a chromosome length of 100 bits. Each parameter (β, γ, λ_r, λ_u, δ) is allotted 20 bits (See Figure 5.1). The mutation rate is set at 0.1, meaning that each bit in a chromosome has a 10% chance of undergoing mutation. We implement flip mutation, where a mutated bit changes its value from 0 to 1 or from 1 to 0. The population size, representing the total number of chromosomes, is set to 100. The algorithm runs for a total of 300 generations. Algorithm of GA shown in Algorithm 1.

We use accuracy metrics RMSE, R-squared, and MAPE are in evaluating the performance of predictive models. RMSE quantifies the average difference between predicted and observed values, providing a measure of the model's precision. R-squared indicates the proportion of variance in the dependent variable explained by the independent variables, reflecting the model's overall goodness of fit. A higher R-squared value suggests a better model fit to the data. MAPE, on the other hand, assesses prediction accuracy in terms of percentage errors relative to the actual values, offering insight into the magnitude of forecasting errors. Lower MAPE values indicate more accurate predictions.

Algorithm 1 Parameter Estimation using Genetic Algorithm for SEIrIuR Model

Import necessary libraries: numpy, scipy, and matplotlib
Define SEIrIuR model function
Define loss function for parameter estimation
Define genetic algorithm functions:
    - initialize_population
    - selection
    - crossover
    - flip_mutation
Define functions for real-to-binary and binary-to-real conversion
Set up parameters for genetic algorithm:
    - population_size
    - chromosome_length
    - mutation_rate
    - generations
Define initial conditions and constants
Initialize population using binary representation
for each generation **do**
        Evaluate fitness for each individual in the population
        Select individuals for reproduction
        Generate new population through crossover and mutation
Convert best solution from binary to real values
Simulate SEIrIuR model with estimated parameters
Plot results
Print estimated parameters and loss
Calculate R-squared and MAPE

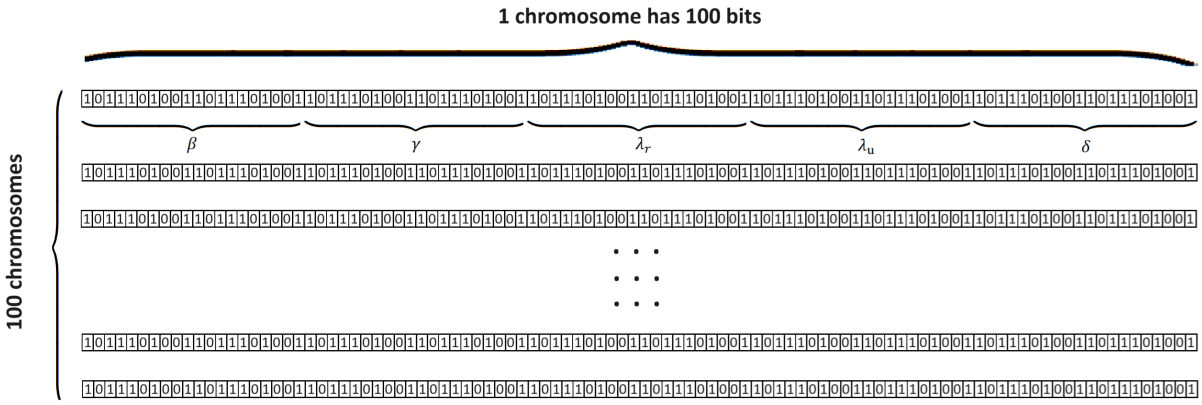

Figure 5.1: Scheme of GA

5.2 Parameter estimation results

Estimated Parameter	Nelder-Mead	L-BFGS-B	Genetic algorithm	HYBRID (GA - NM)	HYBRID (NM - GA)
β	0.865	0.481	0.963	0.997	0.972
γ	0.613	0.114	0.678	0.715	0.598
λ_r	1	0.506	0.953	0.999	0.967
λ_u	0.218	0.01	0.009	0	0.031
δ	0	0.085	0.002	0.001	0.097
$\mathcal{R}_0$	1.41	2.43	1.413	1.391	1.403

Table 5.1: Estimated parameters by Python Odeint and Genetic Algorithm.

Table 5.2 presents a comparison of findings from five different parameter estimation methods using three key metrics: RMSE, R-squared, and MAPE. The GA-NM method achieved the lowest RMSE (605.37), indicating the best fit among the methods, followed by GA (614.399) and NM-GA (612.932). NM and L-BFGS-B had higher RMSE values of 652.375 and 868.946, respectively. The GA, GA-NM, and NM-GA methods all achieved the highest R-squared value of 0.995, demonstrating the best model fit. NM and L-BFGS-B had slightly lower values of 0.994 and 0.991, respectively. L-BFGS-B performed the best with the lowest MAPE (76.867%). Other methods had higher MAPE values, with NM at 119.017%, GA at 135.206%, NM-GA at 135.156%, and GA-NM at 140.789%. To summarize, while GA-NM showed the best performance in terms of RMSE and shared the highest R-squared value with GA and NM-GA, the L-BFGS-B method excelled in terms of MAPE.

- Root Mean Square Error (RMSE) is defined as:

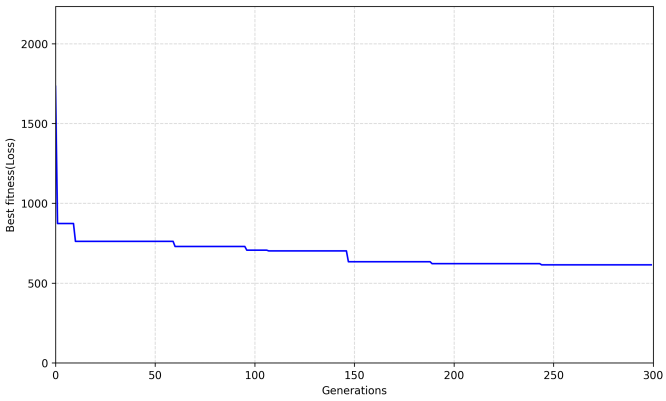

Figure 5.2: Graph of best fitness(loss) GA with 2 parents.

	NM	L-BFGS-B	GA	GA-NM	NM-GA
RMSE	652.375	868.946	614.399	**605.37**	612.932
R-squared	0.994	0.991	**0.995**	**0.995**	**0.995**
MAPE (%)	119.017	**76.867**	135.206	140.789	135.156

Table 5.2: RMSE, R-squared, MAPE comparison between Python Odeint and Genetic Algorithm.

$$RMSE = \sqrt{\frac{1}{n}\sum_{i=1}^{n}(y_i - \hat{y}_i)^2}$$

- The R-squared (R^2) is defined as:

$$R^2 = 1 - \frac{\sum_{i=1}^{n}(y_i - \hat{y}_i)^2}{\sum_{i=1}^{n}(y_i - \overline{y})^2}$$

- Mean Absolute Percentage Error (MAPE) is defined as:

$$MAPE = \frac{100\%}{n}\sum_{i=1}^{n}\left|\frac{y_i - \hat{y}_i}{y_i}\right|$$

where:

- y_i is the actual confirmed value at time i.
- $\hat{y}_i$ is the predicted confirmed value at time i.
- $\overline{y}$ is the mean of the actual confirmed values.
- n is the total number of observations(days).

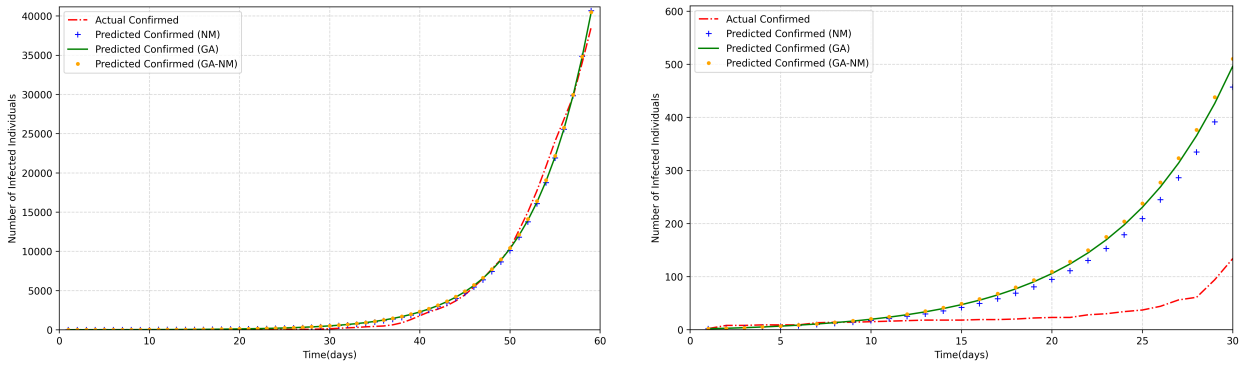

(a) 59 days (b) First 30 days

Figure 5.3: Graphs of actual confirmed cases and model predicted cases are given with NM, GA and GA-NM parameter estimation techniques.

The Q-Q plots Figure 5.5 and histograms Figure 5.4 of the residuals for the SEIrIuR model fitting using five different optimization methods (GA, NM, L-BFGS-B, GA-NM, and NM-GA) reveal notable differences in the performance and distribution of residuals among the methods. The Q-Q plots indicate that all methods exhibit some deviation from normality, particularly at the tails, suggesting the presence of outliers or non-normal residuals. Among the methods, the L-BFGS-B fitting displays the most substantial deviations, especially with extreme negative residuals, as seen in the extended lower tail. The histograms further support these observations, showing that residuals are generally centered around zero for all methods but with varying degrees of spread. GA and NM-GA methods show a tighter concentration of residuals near zero, implying better model fit with fewer extreme errors, whereas L-BFGS-B and NM methods display wider residual distributions, indicating less accurate fits. Overall, while no method achieves perfect normality in residuals, GA and NM-GA provide comparatively better fits to the COVID-19 data, as evidenced by their more centralized residual distributions and fewer outliers.

In Table 5.1 we provide the estimated parameter values for all five different experiments. In all cases we note that the proportion of symptomatic cases (λ_r) are predicted to be higher than asymptomatic cases (λ_u). The graph of Actual Confirmed, Predicted Confirmed by NM and GA is shown in Figure 5.3.

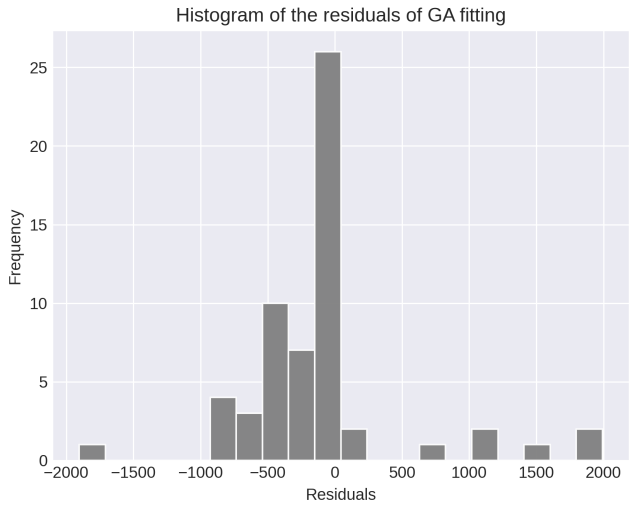

(a) GA

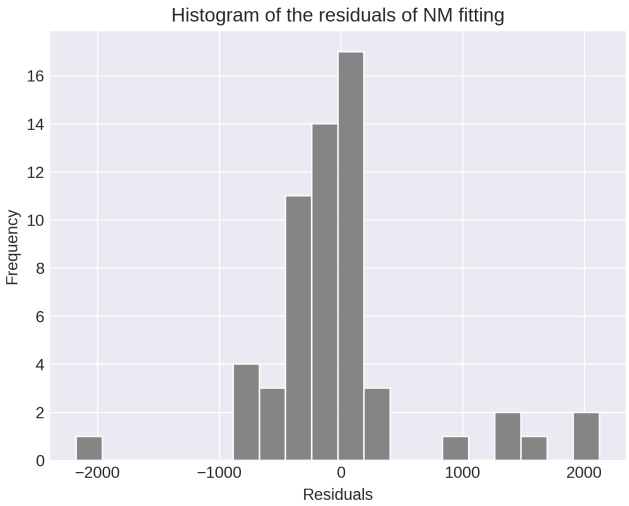

(b) NM

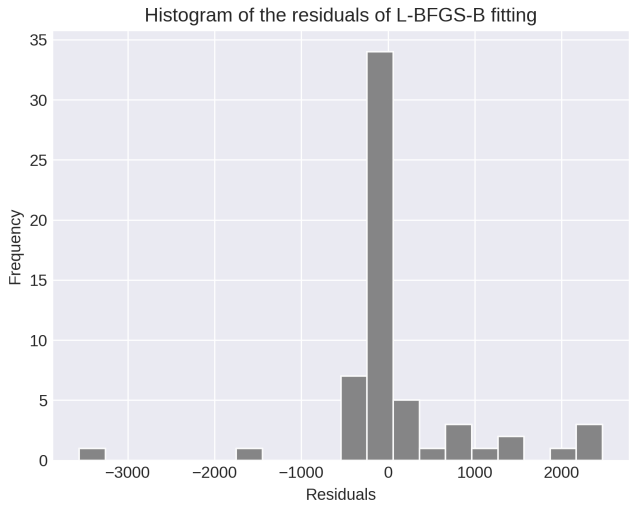

(c) L-BFGS-B

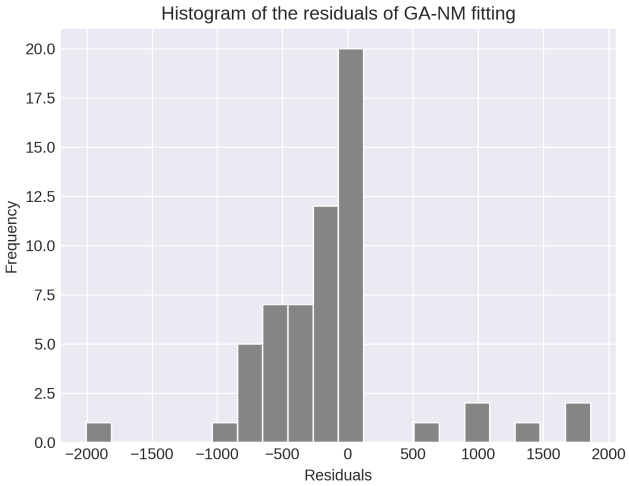

(d) GA-NM

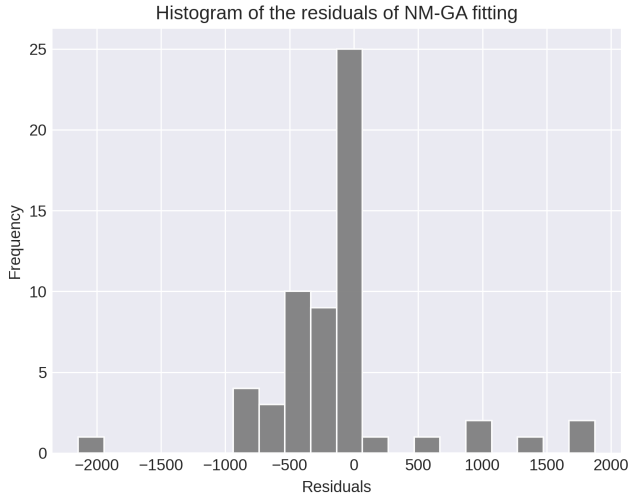

(e) NM-GA

Figure 5.4: Histograms of the residuals of fittings

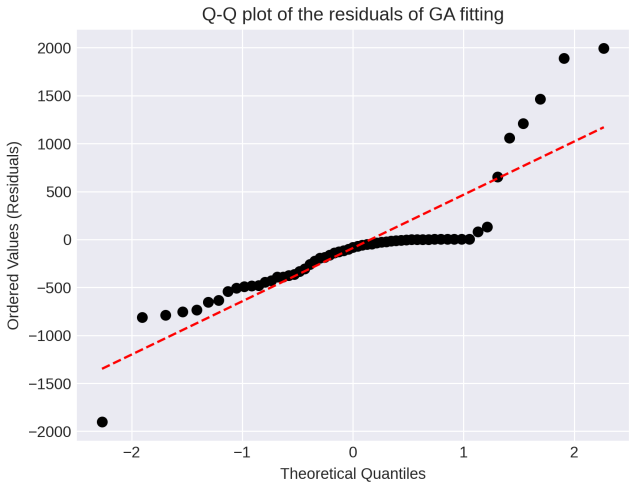

(a) GA

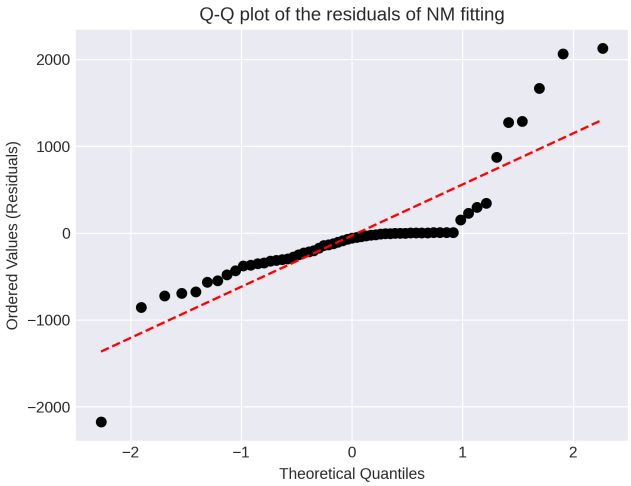

(b) NM

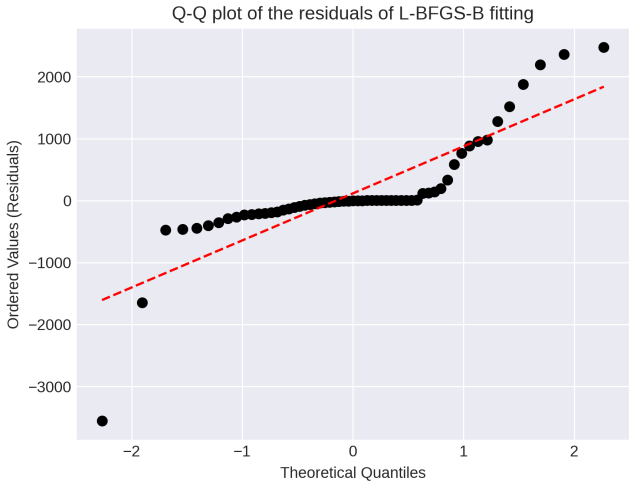

(c) L-BFGS-B

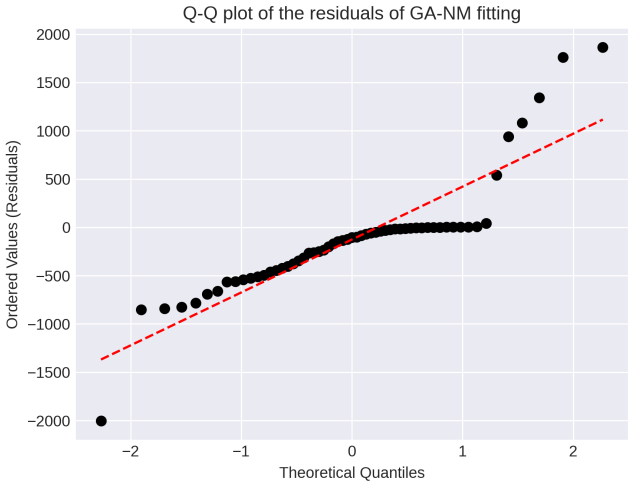

(d) GA-NM

(e) NM-GA

Figure 5.5: Q-Q plots of the residuals of fittings

6. Sensitivity and elasticity analysis

In section, we investigate the dynamics of the SEI_rI_uR model using various analytical techniques. We explore the elasticity of $\mathcal{R}_0$, examine the Partial Rank Correlation Coefficient (PRCC) for parameter influence, and use Sobol indices to prioritize influential factors in the model's output variance, offering insights for intervention strategies.

6.1 Elasticity of $\mathcal{R}_0$

The elasticity of quantity W with respect to a parameter k is given by $\varepsilon_W^k = \frac{\partial W}{\partial k}\frac{k}{W}$, which means the percentage change in W with respect to the percentage change in the parameter k. We are now calculating $\mathcal{R}_0$ elasticity in relation to λ_r and λ_u parameters.

$$\varepsilon_{\mathcal{R}_0}^{\lambda_r} = \frac{\partial \mathcal{R}_0}{\partial \lambda_r}\frac{\lambda_r}{\mathcal{R}_0} = \frac{-\lambda_r(\delta\lambda_u - \gamma\mu - \mu^2)}{(\lambda_r + \lambda_u + \mu)(\delta\lambda_u + (\lambda_r + \lambda_u)(\gamma + \mu)}$$

$$\varepsilon_{\mathcal{R}_0}^{\lambda_u} = \frac{\partial \mathcal{R}_0}{\partial \lambda_u}\frac{\lambda_u}{\mathcal{R}_0} = \frac{\lambda_u(\delta(\lambda_r + \mu) + \gamma\mu + \mu^2)}{(\lambda_r + \lambda_u + \mu)(\delta\lambda_u + (\lambda_r + \lambda_u)(\gamma + \mu)}$$

Here, we observe that the elasticity of $\mathcal{R}_0$ with respect to λ_u is consistently positive due to the positive nature of the parameters involved. However, the elasticity of $\mathcal{R}_0$ concerning λ_r may exhibit both positive and negative values. Specifically, we note that $\varepsilon_{\mathcal{R}_0}^{\lambda_r}$ is negative if $(\delta\lambda_u - \gamma\mu - \mu^2) > 0$. This condition can be expressed equivalently as

$$\varepsilon_{\mathcal{R}_0}^{\lambda_r} < 0 \text{ when } \delta > \frac{\gamma\mu + \mu^2}{\lambda_u}.$$

We can see that in Figure 6.1.

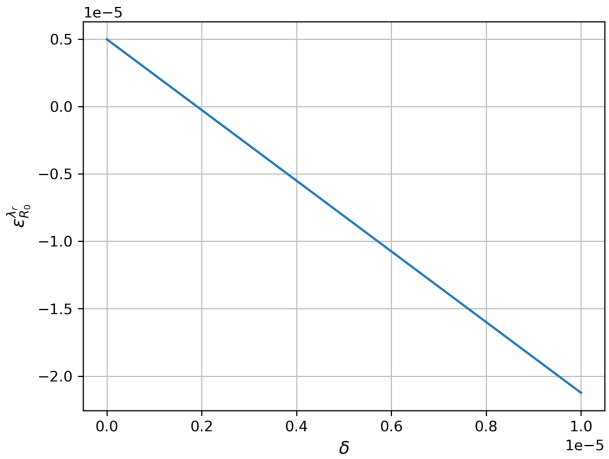

Figure 6.1: $\mathcal{R}_0$ elasticity in relation to λ_r.

6.2 Partial Rank Correlation Coefficient

We examine the sensitivity of our model to various parameters using Partial Rank Correlation Coefficient (PRCC) analysis for time moment $t = 365$. Latin Hypercube Sampling (LHS) generates 4000 parameter combinations. To this end, we defined the following ranges for six key parameters: $\beta, \lambda_u, \lambda_r$ (0.01-0.9), γ (0.01-0.1), δ (0.001-0.1), and α (0.001-0.01). The sensitivity analysis results are visualized in Figure 6.2, depicting the Partial Rank Correlation Coefficient (PRCC) report for compartments E, I_r, I_u, and R. Specifically, the bar charts illustrate the magnitude and directionality of the correlations, complementing the numerical analysis presented earlier. The significance levels are denoted by single, double, and triple asterisks, representing $p < 0.05$, $p < 0.01$, and $p < 0.001$, respectively. The results show that the transmission rate (β) has a strong positive impact across all compartments (E, I_r, I_u, R), as indicated by the high positive PRCC values and statistical significance ($p < 0.001$). Interestingly, while the incubation-adjusted symptomatic (reported) rate (λ_r) exhibits a significant negative correlation with the recovery compartment (R), the asymptomatic rate (λ_u) has a positive effect. This once more emphasizes the importance of introducing symptomatic and asymptomatic compartments separately. Additionally, the rate of losing immunity (α) impacts the disease compartments (E, I_u, I_r) with a magnitude nearly equal to that of the transmission rate (β). Furthermore, the death rate due to the virus (δ) has a significant negative effect on all four compartments. These findings emphasize the critical roles of transmission, recovery, and reporting rates in shaping the dynamics of the SEI_rI_uR model, providing crucial insights for targeted intervention strategies.

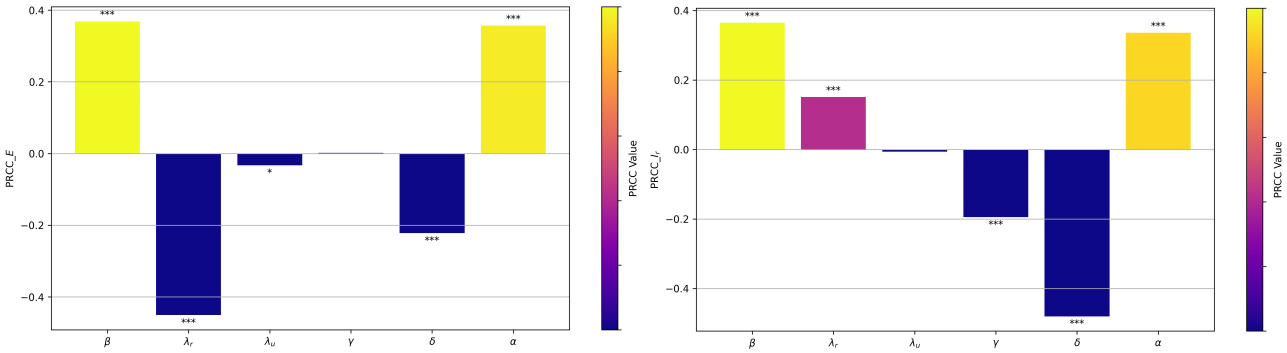

(a) PRCC for E (b) PRCC for I_r

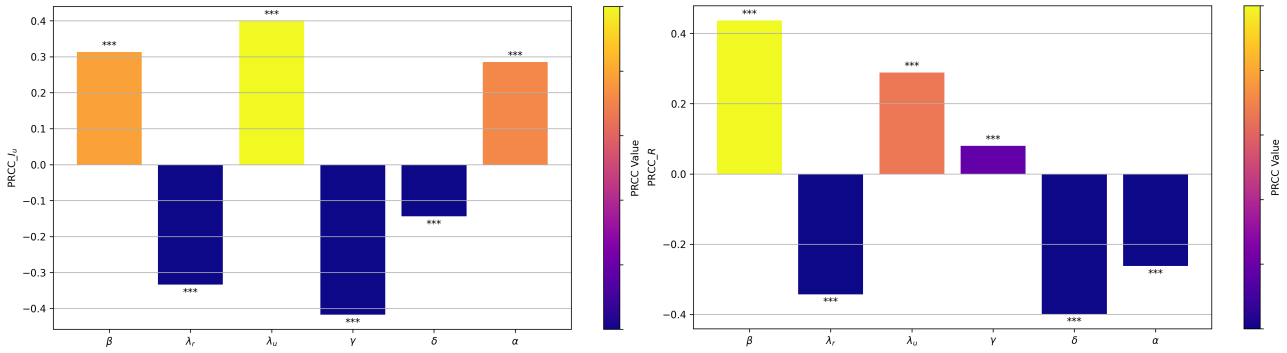

(c) PRCC for I_u (d) PRCC for R

Figure 6.2: PRCC report for compartments E, I_r, I_u, and R.

6.3 Sobel index

In this section, we provide Sobol indices that quantify the contribution of individual input variables or factors to the output variance of a model. It's a sensitivity analysis tool commonly used in Monte Carlo simulations and global sensitivity analyses to prioritize influential factors in complex systems. We set the same parameter ranges as in PRCC and using Saltelli's sampling method, we generated 4096 parameter sets (samples) to ensure robust coverage of the parameter space. The parameter ranges were set as in the previous subsection. The model was then run for 365 days for each parameter set.

The Sobol sensitivity analysis, see Figure 6.3, for the SEI_rI_uR model provides a detailed assessment of the influence of different parameters on the variability of each compartment (E, I_r, I_u, R). The Sobol indices reveal that the transmission rate (β) has the highest impact on the recovered compartment (R), with a Sobol index close to 0.4, indicating a substantial contribution to the variance in R. The recovery rate of unreported infectious individuals (γ) significantly affects the unreported infectious (I_u) and reported infectious (I_r) compartments, with indices around 0.24 and 0.04, respectively. The death due to the virus (δ) is also crucial, predominantly impacting the reported infectious (I_r) and recovered (R) compartments. The rate of loss of immunity (α) has a significant moderate influence on all four compartments with Sobol indices

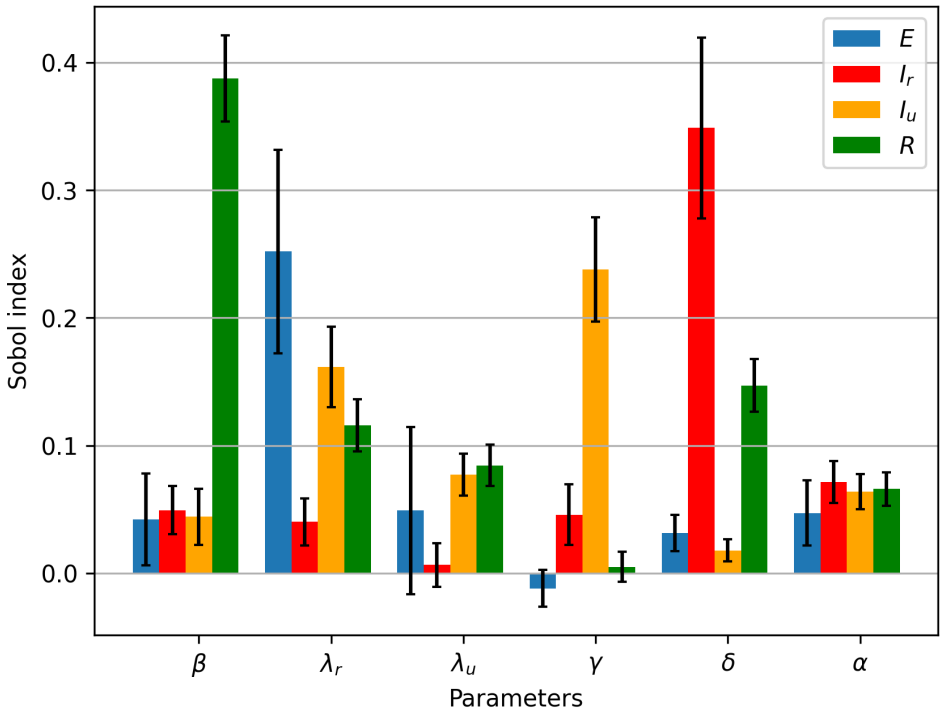

Figure 6.3: Sobol indices for the SEI_rI_uR model parameters.

close to 0.1. These insights highlight the primary drivers of the model's behavior, underscoring the critical roles of transmission, detection, and immunity loss rates in determining the dynamics of the SEI_rI_uR model, and are essential for guiding effective intervention strategies.

7. Visualization

In Fig.7.1, we have plotted various initial values for I, representing the infectious population. As depicted in Fig.7.1, it is evident that irrespective of the initial conditions of I_0, the disease converges to zero. This is attributed to the global stability of the system.

Parameter	Variable	Base value
Total population	N_0	18907256 [40]
Infection rate	β	0.4
Recovery rate	γ	1/14 [41]
Recruitment rate	Λ	419582/365 [40]
Natural death rate	μ	165556/ (365*N_0)
Immunity rate	α	0.7
Average latency period of reported cases	λ_r	0.3
Average latency period of unreported cases	λ_u	0.9
Death rate due to virus	δ	0.015 [42]

Table 7.1: Parameter values corresponding to the model (3.1) in Kazakhstan, for which $\mathcal{R}_0 < 0$

In Fig.7.2, we present a simulation of the system (3.1) using initial conditions reflective of a real-world scenario (specifically, the state of COVID-19 in Kazakhstan on March 13, 2020): $(S, E, I_r, I_u, R) = (18907256, 0, 2, 0, 0)$, with $\mathcal{R}_0 = 3$. The quantity I in Fig.7.2 is the sum of I_r and I_u.

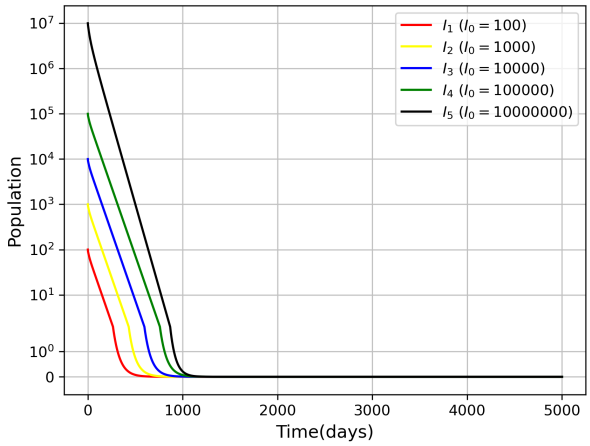

Figure 7.1: Disease dynamics with $\mathcal{R}_0 = 0.8$, $N_0 = 18907256$ and different initial conditions of $I = I_r + I_u$.

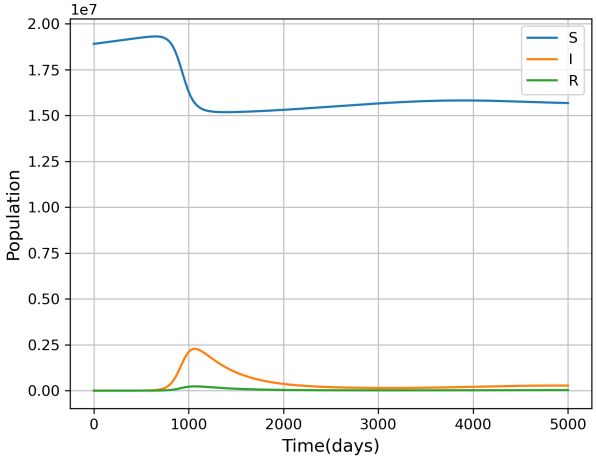

Figure 7.2: Simulation of 3.1 with real situation's initial conditions (COVID-19 in Kazakhstan on 13 March 2020)

8. Conclusion

In conclusion, this study significantly advances biomathematics by introducing a novel epidemic model with separate compartments for symptomatic and asymptomatic cases. Through global stability analysis and parameter estimation using various optimization techniques, including Nelder-Mead, L-BFGS-B, and Genetic Algorithms, we gained insights into disease spread dynamics and accurate parameter estimates. The Genetic Algorithm followed by Nelder-Mead method provided the best fit to the data. Sensitivity analyses, including Partial Rank Correlation Coefficient (PRCC) and Sobol indices, revealed the significant impact of transmission and recovery rates on epidemic dynamics, underscoring the importance of including asymptomatic carriers in models for accuracy. Future research could expand the model to include vaccinated individuals and explore the effects of control measures like social distancing and vaccination campaigns. In summary, this study enhances understanding of epidemic dynamics, informing evidence-based public health decisions and control strategies.

References

[1] Pierre Magal and Shigui Ruan. «Susceptible-infectious-recovered models revisited: from the individual level to the population level.» In: *Mathematical biosciences* 250 (2014), pp. 26–40. URL: https://api.semanticscholar.org/CorpusID:12907445.

[2] Adam T. Biggs and Lanny F. Littlejohn. «How Asymptomatic Transmission Influences Mitigation and Suppression Strategies during a Pandemic». In: *Risk Analysis* (2021). URL: https://api.semanticscholar.org/CorpusID:233483974.

[3] Wenjing Gao et al. «Role of asymptomatic and pre-symptomatic infections in covid-19 pandemic». In: *The BMJ* 375 (2021). URL: https://api.semanticscholar.org/CorpusID:244775641.

[4] Tonglin Sun and Jiangtao Cui. «Modeling the asymptomatic infections for COVID-19 epidemic». In: 2021. URL: https://api.semanticscholar.org/CorpusID:244974585.

[5] Weijie Pang, Hassan Chehaitli, and TR Hurd. «Impact of asymptomatic COVID-19 carriers on pandemic policy outcomes». In: *Infectious Disease Modelling* 7.1 (2022), pp. 16–29.

[6] Xingguang Xingguang Chen Chen. «Infectious Disease Modeling and Epidemic Response Measures Analysis Considering Asymptomatic Infection». In: *Ieee Access* 8 (2020), pp. 149652–149660. URL: https://api.semanticscholar.org/CorpusID:244075430.

[7] Xiaoqi Bi and Carolyn L. Beck. «On the Role of Asymptomatic Carriers in Epidemic Spread Processes». In: *2021 American Control Conference (ACC)* (2021), pp. 3164–3169. URL: https://api.semanticscholar.org/CorpusID:232307334.

[8] Shu Liao and Jin Wang. «Global stability analysis of epidemiological models based on Volterra–Lyapunov stable matrices». In: *Chaos Solitons & Fractals* 45 (2012), pp. 966–977. URL: https://api.semanticscholar.org/CorpusID:120317045.

[9] Jianjun Paul Tian and Jin Wang. «Global stability for cholera epidemic models.» In: *Mathematical biosciences* 232 1 (2011), pp. 31–41. URL: https://api.semanticscholar.org/CorpusID:7253354.

[10] Abderrazak Nabti and Behzad Ghanbari. «Global stability analysis of a fractional SVEIR epidemic model». In: *Mathematical Methods in the Applied Sciences* 44 (2021), pp. 8577–8597. URL: https://api.semanticscholar.org/CorpusID:233975255.

[11] Juping Zhang, Linlin Wang, and Zhen Jin. «Global stability for age-infection-structured human immunodeficiency virus model with heterogeneous transmission». In: *Infectious Disease Modelling* (2024).

[12] Ardak Kashkynbayev, Meruyert Yeleussinova, and Shirali Kadyrov. «An SIRS Pulse Vaccination Model with Nonlinear Incidence Rate and Time Delay». In: *Letters in Biomathematics* 10.1 (2023), pp. 133–148.

[13] Stefania Ottaviano, Mattia Sensi, and Sara Sottile. «Global stability of SAIRS epidemic models». In: *Nonlinear Analysis: Real World Applications* 65 (2022), p. 103501.

[14] Pengcheng Shao and Stanford Shateyi. «Stability analysis of SEIRS epidemic model with nonlinear incidence rate function». In: *Mathematics* 9.21 (2021), p. 2644.

[15] Xiaogang Liu et al. «Global stability of latency-age/stage-structured epidemic models with differential infectivity». In: *Journal of Mathematical Biology* 86.5 (2023), p. 80.

[16] Junling Ma. «Estimating epidemic exponential growth rate and basic reproduction number». In: *Infectious Disease Modelling* 5 (2020), pp. 129–141.

[17] Edoardo Beretta and Yasuhiro Takeuchi. «Global stability of an SIR epidemic model with time delays». In: *Journal of mathematical biology* 33.3 (1995), pp. 250–260.

[18] Andrei Korobeinikov and Graeme C Wake. «Lyapunov functions and global stability for SIR, SIRS, and SIS epidemiological models». In: *Applied Mathematics Letters* 15.8 (2002), pp. 955–960.

[19] Da-peng Gao et al. «Global stability analysis of an SVEIR epidemic model with general incidence rate». In: *Boundary Value Problems* 2018.1 (2018), p. 42.

[20] *sciencedirect.com*. URL: https://www.sciencedirect.com/topics/engineering/lyapunov-stability-theory.

[21] Jean-Jacques E Slotine, Weiping Li, et al. *Applied nonlinear control*. Vol. 199. 1. Prentice hall Englewood Cliffs, NJ, 1991.

[22] A.M. Lyapunov. «The General Problem of the Stability of Motion». In: *Kharkov Mathematical Society, Kharkov* (1892).

[23] BS Goh. «Global stability in two species interactions». In: *Journal of Mathematical Biology* 3.3 (1976), pp. 313–318.

[24] Bo S Goh. «Global stability in many-species systems». In: *The American Naturalist* 111.977 (1977), pp. 135–143.

[25] BS Goh. «Stability in models of mutualism». In: *The American Naturalist* 113.2 (1979), pp. 261–275.

[26] Kuo-Shung Cheng, Sze-Bi Hsu, and Song-Sun Lin. «Some results on global stability of a predator-prey system». In: *Journal of Mathematical Biology* 12.1 (1982), pp. 115–126.

[27] Paul Georgescu and Hong Zhang. «A Lyapunov functional for a SIRI model with nonlinear incidence of infection and relapse». In: *Applied Mathematics and Computation* 219.16 (2013), pp. 8496–8507.

[28] Hongbin Guo, Michael Y Li, and Zhisheng Shuai. «Global dynamics of a general class of multistage models for infectious diseases». In: *SIAM Journal on applied mathematics* 72.1 (2012), pp. 261–279.

[29] Jianquan Li et al. «A class of Lyapunov functions and the global stability of some epidemic models with nonlinear incidence». In: *J. Appl. Anal. Comput* 6.1 (2016), pp. 38–46.

[30] Ruoyan Sun and Junping Shi. «Global stability of multigroup epidemic model with group mixing and nonlinear incidence rates». In: *Applied Mathematics and Computation* 218.2 (2011), pp. 280–286.

[31] Qian Tang, Zhidong Teng, and Xamxinur Abdurahman. «A new Lyapunov function for SIRS epidemic models». In: *Bulletin of the Malaysian Mathematical Sciences Society* 40 (2017), pp. 237–258.

[32] Yerimbet Aitzhanov and Shirali Kadyrov. «TYPES OF LYAPUNOV FUNCTIONS AND GLOBAL STABILITY». In: *SDU Bulletin: Natural and Technical Sciences* 64.1 (2024), pp. 79–88. ISSN: 2709-2631. DOI: 10.47344/sdubnts.v64i1.1179. URL: https://journals.sdu.edu.kz/index.php/nts/article/view/1179.

[33] Cruz Vargas-De-León. «Constructions of Lyapunov functions for classic SIS, SIR and SIRS epidemic models with variable population size». In: *Foro-Red-Mat: Revista electrónica de contenido matemático* 26 (2009), pp. 1–12.

[34] Pauline Van den Driessche and James Watmough. «Reproduction numbers and sub-threshold endemic equilibria for compartmental models of disease transmission». In: *Mathematical biosciences* 180.1-2 (2002), pp. 29–48.

[35] Yan Bai et al. «Presumed asymptomatic carrier transmission of COVID-19». In: *Jama* 323.14 (2020), pp. 1406–1407.

[36] Benjamin Ivorra et al. «Mathematical modeling of the spread of the coronavirus disease 2019 (COVID-19) taking into account the undetected infections. The case of China». In: *Communications in nonlinear science and numerical simulation* 88 (2020), p. 105303.

[37] Santosh Ansumali et al. «Modelling a pandemic with asymptomatic patients, impact of lockdown and herd immunity, with applications to SARS-CoV-2». In: *Annual reviews in control* 50 (2020), pp. 432–447.

[38] Ensheng Dong, Hongru Du, and Lauren Gardner. «An interactive web-based dashboard to track COVID-19 in real time». In: *The Lancet infectious diseases* 20.5 (2020), pp. 533–534.

[39] Statista. *UK population data from 1887 to 2021*. `https://www.statista.com/statistics/281488/number-of-deaths-in-the-united-kingdom-uk/`. [Accessed: May 17, 2024]. 2020.

[40] Bureau of National Statistics. *Official Website of the Bureau of National Statistics*. `https://stat.gov.kz/`. Accessed: January 5, 2022.

[41] Hozaifa Khalil Elsawah et al. «Efficacy and safety of remdesivir in hospitalized Covid-19 patients: systematic review and meta-analysis including network meta-analysis». In: *Reviews in medical virology* 31.4 (2021), e2187.

[42] Athanasios-Dimitrios Bakasis et al. «COVID-19 infection among autoimmune rheumatic disease patients: data from an observational study and literature review». In: *Journal of Autoimmunity* 123 (2021), p. 102687.